Cooperative NOMA-Based DCO-OFDM VLC System

Xin Liu[1(✉)], Yuyao Wang[2], and Zhenyu Na[2]

[1] School of Information and Communication Engineering, Dalian University of Technology, Dalian 116024, China
liuxinstar1984@dlut.edu.cn

[2] School of Information Science and Technology, Dalian Maritime University, Dalian 116026, China

Abstract. In this paper, relaying technique and non-orthogonal multiple access (NOMA) are adopted to improve performance of visible light communication (VLC) system. Due to the adoption of relay terminal, the link reliability and communication coverage of VLC system are boosted. Besides, the utilization of NOMA can greatly increase spectral efficiency and support massive connectivity. So, a cooperative NOMA-based DCO-OFDM VLC system is proposed. All the optical transmission links use DCO-OFDM to accomplish information transmission. The relay terminal in the proposed system not only forwards the source signal but also sends its own signal simultaneously. The signals over the links between relay and two users are superposed based on NOMA. Under different cases, the total throughput is analyzed and the optimal power allocation factor is obtained. In addition, the OMA-based system is taken as the benchmark system. The simulation results further verify the theoretical results and the superiority that the proposed system has.

Keywords: Relay · NOMA · VLC · DCO-OFDM

1 Introduction

In recent days, the requirements for wireless communication achieve explosive growth. As a result, the available spectrum resources are getting more and more tense. Thus, communication techniques need to be innovated and improved. Visible light communication (VLC) has emerged as one of the promising solutions for indoor high-speed transmission, which can realize illumination and communication simultaneously [1]. VLC has free and wide optical spectrum, high secrecy and security, and low-cost implementation, so it has attracted significant interests. In VLC system, OFDM is one of the most commonly used technologies to decrease the bit error rate (BER). There are some typical VLC schemes based on OFDM have been put forward, such as DCO-OFDM, ACO-OFDM, PAM-DMT, PM-OFDM, U-OFDM and ADO-OFDM [2–4]. Compared with other systems,

J. Jin et al. (Eds.): GreeNets 2019, LNICST 282, pp. 14–24, 2019.
https://doi.org/10.1007/978-3-030-21730-3_2

DCO-OFDM is easier to achieve and has lower cost. So, DCO-OFDM is used in all the transmission links of our proposed system.

There are always some obstacles such as furniture and home appliances in the application scenes of VLC network. The existence of these obstacles may block the light. And then, the information transmission will be interrupted. Besides, the signals will suffer great attenuation when the distance between the light emitting diode (LED) and photodiode (PD) is too far. The application of relaying technique in VLC system can compensate this weakness. Cooperative VLC system has stronger link reliability and wider communication coverage than traditional VLC system [5]. Therefore, it has attracted wide attention of many scholars. [6] shows the performance improvement that amplify-and-forward (AF) and decode-and-forward (DF) relay brought to VLC system. [7] demonstrates the superiority of full-duplex (FD) relay-assisted VLC system over half-duplex (HD) relay-assisted VLC system in BER performance.

Non-orthogonal multiple access (NOMA) technique is a promising candidate for 5G multiple access techniques. Compared with orthogonal multiple access (OMA), NOMA supports more users at the same time [8]. In the power-domain NOMA method, more transmission power is allocated to the user with poorer channel condition, while less power is allocated to the user with better channel condition [9]. Then, the signals from various users are superposed together and sent to receiver side. At receiver side, the superposed signals are de-multiplexed by using serial interference cancellation (SIC) [10]. Nowadays, there are some researches on the application of NOMA to VLC system. [11] proposes a NOMA-DCO-OFDM system and shows its superiority over OMA-DCO-OFDM system. [12] and [13] also make performance evaluation of NOMA in VLC system and reveal its performance gain over OMA system.

However, there are few studies on the joint application of relaying technique and NOMA in VLC system. Therefore, we propose a cooperative NOMA-based DCO-OFDM VLC system. The system uses DF relay to forward the signal from source terminal. By using NOMA, the relay terminal not only forwards the source signal, but also transmits relay signal to corresponding destination terminal. The optimal power allocation factor is obtained by maximizing the system throughput. In addition, the superiority of NOMA-based system over OMA-based system is also verified.

2 System Model

Consider a typical office space with one main light source (S) at the ceiling, one relay terminal (R) at the desk, and two destination terminals (U and D) closer to R. The cooperative NOMA-based DCO-OFDM VLC system is shown in Fig. 1. S and R are equipped with LED units to convert electrical signals to optical signals and send them out, while R, U and D are equipped with PD to convert optical signals to electrical signals for demodulation. There are two independent time slots in the proposed system. As Fig. 1 shows, the blue line represents the first time slot, while the red lines represent the second time slot.

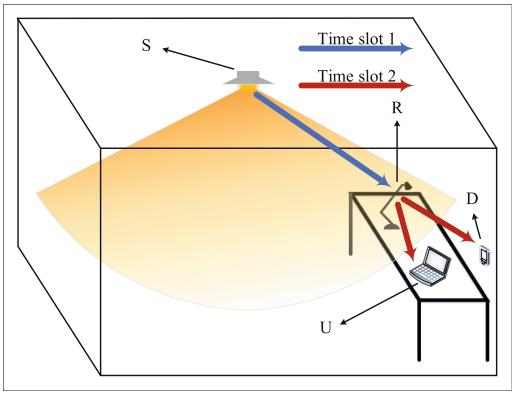

Fig. 1. System model.

During the first time slot, the bit streams are encoded and modulated at S and S sends the modulated signals to R. Then, R receives and decodes the bits that S transmits. During the second time slot, the source signals decoded at R are encoded again. The re-encoded signals are sent out by R with the relay signals together. These two kinds of signals are superposed in power domain according to NOMA and they use the same frequency band at the same time. U and D receive the superposed signals and decode the signals to obtain the transmission bit streams of S and R, respectively.

A cooperative OMA-based DCO-OFDM VLC system is taken as the benchmark system in this paper. Different from the transmission based on NOMA, the re-encoded signals and relay signals in the benchmark system share the frequency band and each of them uses half the bandwidth. The sub-bands they used are orthogonal to each other. The comparison of throughput between these two systems are discussed in the following sections.

3 Model Analysis

In the proposed system, the total transmission power of S and R is constrained to P_t and the transmission power of S and R are set to be the same, i.e. $P_S = P_R = \frac{1}{2}P_t$. Because of the adoption of DCO-OFDM scheme in the four links, we use the model of non-linear clipping operation in [11]. The signal sent from transmitter to receiver is double-sided clipped. Then, DC bias is added to the clipped signal to make the signal be positive signal. Supposing that the signal transmitted by S is x, while the signal after non-linear clipping process is x_{clip}. x is a Gaussian random signal whose mean $\mu_x = 0$ and variance $\sigma_x^2 = P_S$. In this section, we first introduce the clipping model of S-to-R link. Then, the total throughput of the signals received by U and D during the second time slot is deduced. Finally, the comparison of the total throughput of U and D between the NOMA-based and OMA-based systems is given.

3.1 Clipping Model

The non-linear double-sided clipping operation of DCO-OFDM scheme is defined as

$$C_1(x) = \begin{cases} \lambda_t^S - B_{dc}^S & x > \lambda_t^S - B_{dc}^S \\ x & \lambda_b^S < x < \lambda_t^S \\ \lambda_b^S - B_{dc}^S & x < \lambda_b^S - B_{dc}^S \end{cases} \tag{1}$$

where λ_t^S and λ_b^S are the upper and lower boundaries of the clipping operation at S, respectively. B_{dc}^S is the DC bias of the non-linear clipping operation at S. According to Bussgang Theorem, x_{clip} can be divided into two parts as follows [11].

$$x_{clip} = a_S x + d_S \tag{2}$$

where a_S and d_S are the attenuation factor and clipping noise caused by the non-linear clipping operation at S. According to Bussgang Theorem, a_S can be calculated by

$$a_S = \frac{1}{2}\text{erf}\left(\frac{l_S}{\sqrt{2}}\right) - \frac{1}{2}\text{erf}\left(\frac{m_S}{\sqrt{2}}\right) \tag{3}$$

where $l_S = \frac{\lambda_t^S - B_{dc}^S}{\sigma_x}$ and $m_S = \frac{\lambda_b^S - B_{dc}^S}{\sigma_x}$. d_S is usually a Gaussian random noise with non-zero mean and it can be divided into two separate parts as

$$d_S = \mu_S + \mathbb{E}\left[d_S\right] \tag{4}$$

where $\mathbb{E}\left[d_S\right]$ means the operation to get the mean value of d_S. μ_S is a zero-mean random variable uncorrelated with x. According to (4), the power of clipping noise $P_{clip}^S = \mathbb{D}\left[d_S\right] = \mathbb{E}\left[\mu_S^2\right]$, where $\mathbb{D}\left[d_S\right]$ is the operation to get the variance of d_S. By substituting (4) into (2), P_{clip}^S is obtained as

$$P_{clip}^S = \mathbb{E}\left[x_{clip}^2\right] - a_S^2\mathbb{E}\left[x^2\right] - \mathbb{E}\left[d_S\right]^2 \tag{5}$$

Therefore, the calculation of P_{clip}^S is converted to be the calculation processes of $\mathbb{E}[x_{clip}^2]$ and $\mathbb{E}[d_S]$. According to (1), the probability density function of x_{clip} can be obtained. So, the expressions of $\mathbb{E}[x_{clip}^2]$ and $\mathbb{E}[d_S]$ can be obtained as follows.

$$\begin{aligned} \mathbb{E}\left[x_{clip}^2\right] = \frac{\sigma_x^2}{2}\Bigg[& l_S^2 + m_S^2 - \left(l_S^2 - 1\right)\text{erf}\left(\frac{l_S}{\sqrt{2}}\right) \\ & + \left(m_S^2 - 1\right)\text{erf}\left(\frac{m_S}{\sqrt{2}}\right) + 2m_S g\left(m_S\right) - 2l_S g\left(l_S\right)\Bigg] \end{aligned} \tag{6}$$

$$\mathbb{E}\left[d_S\right] = \frac{\sigma_x}{2}\left[l_S + m_S - l_S\text{erf}\left(\frac{l_S}{\sqrt{2}}\right) + m_S\text{erf}\left(\frac{m_S}{\sqrt{2}}\right) + 2g\left(m_S\right) - 2g\left(l_S\right)\right] \tag{7}$$

And $\mathbb{E}[x^2] = \sigma_x^2$, according to (3), (6) and (7), P_{clip}^S can be rewritten as

$$\begin{aligned} P_{clip}^S &= \frac{\sigma_x^2}{2}\left[m_S^2 + 2m_S g(m_S) + (m_S^2 - 1)\mathrm{erf}(\frac{m_S}{\sqrt{2}}) + l_S^2 - (l_S^2 - 1)\mathrm{erf}(\frac{l_S}{\sqrt{2}}) - 2l_S g(l_S)\right] \\ &\quad - \left\{\frac{\sigma_x}{2}\left[l_S + m_S - l_S\mathrm{erf}(\frac{l_S}{\sqrt{2}}) + m_S\mathrm{erf}(\frac{m_S}{\sqrt{2}}) + 2g(m_S) - 2g(l_S)\right]\right\}^2 - a_S^2\sigma_x^2 \end{aligned} \tag{8}$$

3.2 Throughput Analysis

The signal received by R during the first time slot is expressed as

$$z_1 = h_1 * (x_{clip} + B_{dc}^S) + n_1 \tag{9}$$

According to DCO-OFDM, B_{dc}^S only affects the DC signal, not the power of useful signal. So, substituting (2) into (9), the signal-to-noise ratio (SNR) of z_1 is expressed by

$$\gamma_1 = \frac{|h_1|^2 a_S^2 \sigma_x^2}{|h_1|^2 P_{clip}^S + \sigma_n^2} \tag{10}$$

where σ_n^2 is variance of channel noise n_1. In this paper, all channel noises are seen as Gaussian random signals with zero-mean and variance σ_n^2. So, the throughput of the signals transmitted from S to R during the first time slot is

$$T_1 = \frac{1}{2}\log_2(1 + \gamma_1) = \frac{1}{2}\log_2\left(1 + \frac{|h_1|^2 a_S^2 \sigma_x^2}{|h_1|^2 P_{clip}^S + \sigma_n^2}\right) \tag{11}$$

To simplify the discussion, the relay terminal R is assumed to decode the signal transmitted from S successfully. During the second time slot, the decoded source signal and relay signal are superposed together in the power domain based on NOMA. The signals transmitted by R to both D and U are consisted of two independent parts: the decoded source signal y_1 and relay signal y_2. y_1 and y_2 are both Gaussian random signals whose mean values are zero and variances are 1. So, the transmitted superposed signal in R-to-U and R-to-D links is expressed as follows

$$y = \sqrt{(1-\beta)P_R}y_1 + \sqrt{\beta P_R}y_2 \tag{12}$$

where β is the power allocation factor between R-to-U and R-to-D links during the second time slot. Denoting that the superposed signal transmitted by R after clipping operation is y_{clip}, the non-linear double-sided clipping operation at R is given by

$$C_2(y) = \begin{cases} \lambda_t^R - B_{dc}^R & y > \lambda_t^R - B_{dc}^R \\ y & \lambda_b^R < y < \lambda_t^R \\ \lambda_b^R - B_{dc}^R & y < \lambda_b^R - B_{dc}^R \end{cases} \tag{13}$$

where λ_t^R and λ_b^R are the upper and lower boundaries of the double-sided clipping operation at R, respectively. B_{dc}^R is the DC bias of the clipping operation at R. According to Bussgang Theorem, y_{clip} can be modeled as

$$y_{clip} = a_R y + d_R \tag{14}$$

where a_R and d_R are the attenuation factor and clipping noise caused by the nonlinear clipping operation, respectively. Correspondingly, a_R can be calculated by

$$a_R = \frac{1}{2}\text{erf}\left(\frac{l_R}{\sqrt{2}}\right) - \frac{1}{2}\text{erf}\left(\frac{m_R}{\sqrt{2}}\right) \tag{15}$$

where $l_R = \frac{\lambda_t^R - B_{dc}^R}{\sigma_y}$ and $m_R = \frac{\lambda_b^R - B_{dc}^R}{\sigma_y}$, $\sigma_y^2 = P_R$ is the variance of y. Similar to d_S, d_R is a Gaussian random noise with non-zero mean and it can be divided into two separate parts as

$$d_R = \mu_R + \mathbb{E}[d_R] \tag{16}$$

where $\mathbb{E}[d_R]$ is the mean value of d_R, μ_R is a zero mean random variable uncorrelated with y. Thus, the power of the clipping noise y_{clip} is $P_{clip}^R = \mathbb{D}[d_R] = \mathbb{E}[\mu_R^2]$. By substituting (16) into (14), P_{clip}^R can be rewritten as

$$P_{clip}^R = \mathbb{E}[\mu_R^2] = \mathbb{E}[y_{clip}^2] - a_R^2\mathbb{E}[y^2] - \mathbb{E}[d_R]^2 - 2a_R\mathbb{E}[y]\,\mathbb{E}[d_R] \tag{17}$$

Similar to the calculation of P_{clip}^S, the result of (17) can be obtained as

$$\begin{aligned} &P_{clip}^R \\ &= \frac{\sigma_y^2}{2}\left[m_R^2 + 2m_R g(m_R) + (m_R^2 - 1)\text{erf}(\frac{m_R}{\sqrt{2}}) + l_R^2 - (l_R^2 - 1)\text{erf}(\frac{l_R}{\sqrt{2}}) - 2l_R g(l_R)\right] \\ &\quad - \left\{\frac{\sigma_y}{2}\left[l_R + m_R - l_R\text{erf}(\frac{l_R}{\sqrt{2}}) + m_R\text{erf}(\frac{m_R}{\sqrt{2}}) + 2g(m_R) - 2g(l_R)\right]\right\}^2 - a_R^2\sigma_y^2 \end{aligned} \tag{18}$$

The signals received by U and D during the second time slot are respectively expressed as follows

$$\begin{aligned} z_2 &= h_2 * (y_{clip} + B_{dc}^R) + n_2 \\ z_3 &= h_3 * (y_{clip} + B_{dc}^R) + n_3 \end{aligned} \tag{19}$$

where h_2 and h_3 mean the channel gains of R-to-U and R-to-D links, respectively. y_{clip} is the clipping signal transmitted from R to both U and D. n_2 and n_3 are the channel noises of R-to-U link and R-to-D link, respectively.

Supposing that $h_2 > h_3$, based on the demodulation principle of NOMA, the SNR of U and D are respectively calculated as

$$\gamma_2 = \frac{|h_2|^2 a_R^2 (1-\beta) P_R}{|h_2|^2 P_{clip}^R + \sigma_n^2} \tag{20}$$

$$\gamma_3 = \frac{|h_3|^2 a_R^2 \beta P_R}{|h_3|^2 P_{clip}^R + |h_3|^2 a_R^2 (1-\beta) P_R + \sigma_n^2} \tag{21}$$

The throughput of the signals transmitted from R to U during the second time slot is expressed by

$$T_2 = \frac{1}{2}\log_2\left(1+\gamma_2\right) = \frac{1}{2}\log_2\left(1+\frac{\left|h_2\right|^2 a_R^2\left(1-\beta\right)P_R}{\left|h_2\right|^2 P_{clip}^R+\sigma_n^2}\right) \tag{22}$$

Since DF relay is adopted in this system, the total throughput of the source signal is

$$T_S = \min\left(T_1, T_2\right) \tag{23}$$

In addition, the throughput of signal transmitted from R to D during the second time slot is

$$T_R = \frac{1}{2}\log_2\left(1+\gamma_3\right) = \frac{1}{2}\log_2\left(1+\frac{\left|h_3\right|^2 a_R^2\beta P_R}{\left|h_3\right|^2 P_{clip}^R+\left|h_3\right|^2 a_R^2\left(1-\beta\right)P_R+\sigma_n^2}\right) \tag{24}$$

Moreover, as a benchmark, the SNR of the signals received by U and D during the second time slot in the OMA-based system are expressed as

$$\widetilde{\gamma}_2 = \frac{\left|h_2\right|^2 a_R^2\left(1-\beta\right)P_R}{\left|h_2\right|^2 P_{clip}^R+\sigma_n^2} \tag{25}$$

$$\widetilde{\gamma}_3 = \frac{\left|h_3\right|^2 a_R^2\beta P_R}{\left|h_3\right|^2 P_{clip}^R+\sigma_n^2} \tag{26}$$

Then, the total throughput of source signal in the benchmark system is given as follows

$$\widetilde{T}_S = \min\left(\frac{1}{2}\log_2\left(1+\gamma_1\right), \frac{1}{4}\log_2\left(1+\widetilde{\gamma}_2\right)\right) \tag{27}$$

The throughput of signal transmitted from R to D during the second time slot is

$$\widetilde{T}_R = \frac{1}{4}\log_2\left(1+\widetilde{\gamma}_3\right) = \frac{1}{4}\log_2\left(1+\frac{\left|h_3\right|^2 a_R^2\beta P_R}{\left|h_3\right|^2 P_{clip}^R+\sigma_n^2}\right) \tag{28}$$

4 Simulations and Discussions

In the previous sections, the throughput performance of the system have been theoretically analyzed. According to the theoretical deduction, we analyze the throughput with different parameters by simulation in this section. Some parameters used in the simulation are set as follows, the total power of S and R $P_t = 26\,\mathrm{W}$, the transmission power of S and R $P_S = P_R = 13\,\mathrm{W}$, $\lambda_t^S = 7\,\mathrm{V}$, $\lambda_t^R = 5\,\mathrm{V}$, $\lambda_b^S = \lambda_b^R = 0\,\mathrm{V}$ and power of noise $P_n = \sigma_n^2 = 1\,\mathrm{W}$.

Figure 2 shows the total throughput of signals transmitted to both U and D during the second time slot with varying power allocation factor β. It is seen that $T_S + T_R$ first increases and then decreases with the increase of β. When B_{dc}^R is

too small, the clipping noise is too big. So $T_S + T_R$ is small at the beginning and increases with B_{dc}^R. However, when B_{dc}^R reaches to a certain value, it will waste many power. Correspondingly, the useful power will get smaller, so $T_S + T_R$ stops increasing and begins to decrease with the increase of B_{dc}^R. There is an optimal B_{dc}^R to maximize $T_S + T_R$ no matter what β is. Figure 2 also shows that the performance is the same when the sum of two β equals to 1. In this section, we set $h_2 = 0.9, h_3 = 0.6$ when $h_2 > h_3$ and $h_2 = 0.6, h_3 = 0.9$ when $h_2 < h_3$. Therefore, the theoretical expressions are symmetric and the throughput results are the same when the sum of two β equals to 1.

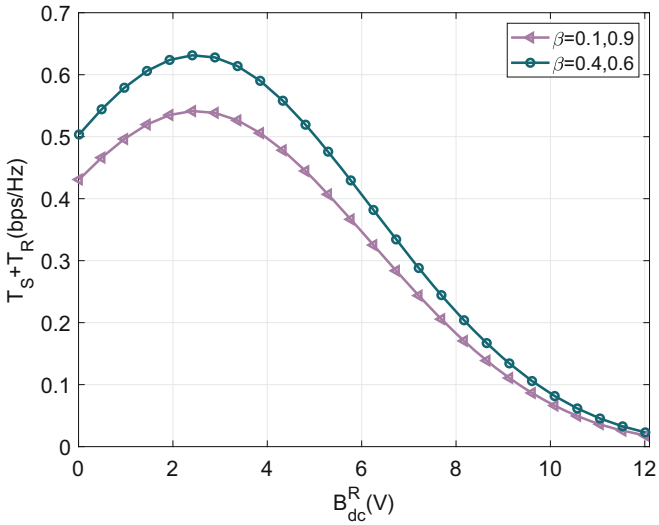

Fig. 2. The total throughput of U and D during the second time slot with varying B_{dc}^R.

Figure 3 shows the throughput performance with varying β. It can be seen that $T_S + T_R$ first increases and then decreases, and it reaches its maximum at $\beta = 0.5$. When $\beta < 0.5$, the increase of β means the increase of power allocated to D with better channel condition. As well, when $\beta > 0.5$, the increase of β means the decrease of power allocated to U with better channel condition. Therefore, $T_S + T_R$ increases with the increase of β when $\beta < 0.5$. On the other hand, $T_S + T_R$ decreases with the increase of β when $\beta > 0.5$, i.e., when the power allocated to the user with better channel condition increases, the throughput performance gets better. So, when $\beta = 0.5$, the power allocated to the user with better channel gets its maximum value and the throughput performance reaches its maximum value.

Figure 4 shows the comparison of the throughput performance between the proposed NOMA-based system and the benchmark system based on OMA. It can be seen that with the increase of β, the trend of the throughput curve of OMA-based system is the same as the one of NOMA-based system. Furthermore, the

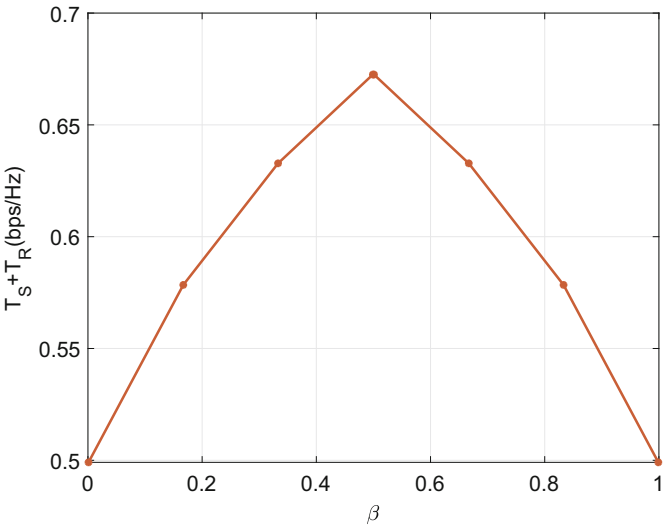

Fig. 3. The throughput performance with varying β during the second time slot.

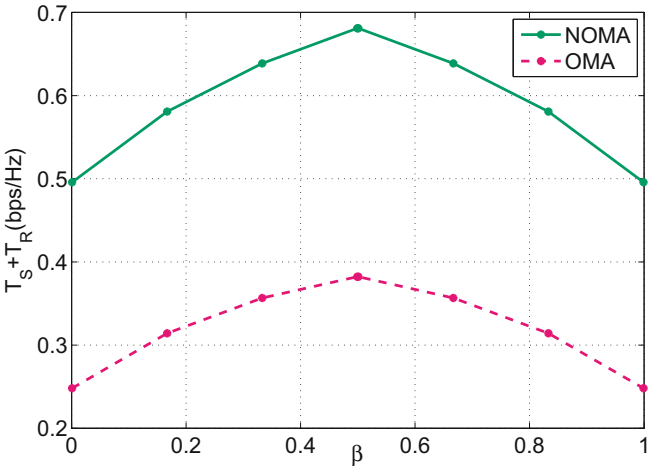

Fig. 4. The comparison of throughput performance with varying β between NOMA-based and OMA-based system.

introduction of NOMA improves the system throughput performance in general. Because the spectrum efficiency of OMA-based system is almost half of that in NOMA-based system. The total throughput of NOMA-based system is almost twice the throughput of the benchmark system based on OMA.

5 Conclusion

In this paper, a cooperative NOMA-based DCO-OFDM VLC system is proposed and analyzed. In the proposed system, all the transmission links use DCO-OFDM scheme to transmit signal. The DF relay terminal forwards the source signal and transmits relay signal to corresponding destination terminals at the same time. These two kinds of signals are superposed in the power domain based on NOMA. The clipping noise and total throughput are modeled and analyzed. The simulation results show that when the power allocated to the user with better channel condition increases during the second time slot, the total throughput increases. So, the selection of appropriate value of the power allocation factor is necessary for the system performance. Besides, the comparison between the proposed system based on NOMA and the benchmark system based on OMA reveals the performance gain that NOMA brings to the system.

Acknowledgements. This work was supported by the National Natural Science Foundations of China under Grant 61601221, the Joint Foundations of the National Natural Science Foundations of China and the Civil Aviation of China under Grant U1833102, and the China Postdoctoral Science Foundations under Grants 2015M580425 and 2018T110496.

References

1. Grobe, L., et al.: High-speed visible light communication systems. IEEE Commun. Mag. **51**(12), 60–66 (2013)
2. Elgala, H., Mesleh, R., Haas, H.: Indoor broadcasting via white LEDs and OFDM. IEEE Trans. Consum. Electron. **55**(3), 1127–1134 (2009)
3. Armstrong, J., Lowery, A.J.: Power efficient optical OFDM. Electron. Lett. **42**(6), 370–372 (2006)
4. Dissanayake, S.D., Panta, K., Armstrong, J.: A novel technique to simultaneously transmit ACO-OFDM and DCO-OFDM in IM/DD systems. In: 2011 IEEE GLOBECOM Workshops (GC Wkshps), pp. 782–786, December 2011
5. Kizilirmak, R.C., Uysal, M.: Relay-assisted OFDM transmission for indoor visible light communication. In: 2014 IEEE International Black Sea Conference on Communications and Networking (BlackSeaCom), pp. 11–15, May 2014
6. Yang, H., Pandharipande, A.: Full-duplex relay VLC in LED lighting linear system topology. In: IECON 2013 - 39th Annual Conference of the IEEE Industrial Electronics Society, pp. 6075–6080, November 2013
7. Narmanlioglu, O., Kizilirmak, R.C., Miramirkhani, F., Uysal, M.: Cooperative visible light communications with full-duplex relaying. IEEE Photonics J. **9**(3), 1–11 (2017)
8. Dai, L., Wang, B., Ding, Z., Wang, Z., Chen, S., Hanzo, L.: A Survey of non-orthogonal multiple access for 5G. IEEE Commun. Surv. Tutor. **20**, 2294–2323 (2018)
9. Ding, Z., Fan, P., Poor, H.V.: Impact of user pairing on 5G nonorthogonal multiple-access downlink transmissions. IEEE Trans. Veh. Technol. **65**(8), 6010–6023 (2016)
10. Ding, Z., Lei, X., Karagiannidis, G.K., Schober, R., Yuan, J., Bhargava, V.K.: A survey on non-orthogonal multiple access for 5G networks: research challenges and future trends. IEEE J. Sel. Areas Commun. **35**(10), 2181–2195 (2017)

11. Chu, W., Dang, J., Zhang, Z., Wu, L.: Effect of clipping on the achievable rate of non-orthogonal multiple access with DCO-OFDM. In: 2017 9th International Conference on Wireless Communications and Signal Processing (WCSP), pp. 1–6. IEEE (2017)
12. Yin, L., Wu, X., Haas, H.: On the performance of non-orthogonal multiple access in visible light communication. In: 2015 IEEE 26th Annual International Symposium on Personal, Indoor, and Mobile Radio Communications (PIMRC), pp. 1354–1359, August 2015
13. Yin, L., Popoola, W.O., Wu, X., Haas, H.: Performance evaluation of non-orthogonal multiple access in visible light communication. IEEE Trans. Commun. **64**(12), 5162–5175 (2016)